NIGHT-TIME DEHAZING BY FUSION

Cosmin Ancuti [*‡], *Codruta O. Ancuti* [†‡], *Christophe De Vleeschouwer* [*] *and Alan C. Bovik* [§]

[*] ICTEAM, Universite Catholique de Louvain, Belgium
[†] Computer Vision and Robotics Group, University of Girona, Spain
[‡] MEO, Universitatea Politehnica Timisoara, Romania
[§] Department of Electrical and Computer Engineering, The University of Texas at Austin, USA

ABSTRACT

We introduce an effective technique to enhance night-time hazy scenes. Our technique builds on multi-scale fusion approach that use several inputs derived from the original image. Inspired by the dark-channel [1] we estimate night-time haze computing the airlight component on image patch and not on the entire image. We do this since under night-time conditions, the lighting generally arises from multiple artificial sources, and is thus intrinsically non-uniform. Selecting the size of the patches is non-trivial, since small patches are desirable to achieve fine spatial adaptation to the atmospheric light, this might also induce poor light estimates and reduced chance of capturing hazy pixels. For this reason, we deploy multiple patch sizes, each generating one input to a multiscale fusion process. Moreover, to reduce the glowing effect and emphasize the finest details, we derive a third input. For each input, a set of weight maps are derived so as to assign higher weights to regions of high contrast, high saliency and small saturation. Finally the derived inputs and the normalized weight maps are blended in a multi-scale fashion using a Laplacian pyramid decomposition. The experimental results demonstrate the effectiveness of our approach compared with recent techniques both in terms of computational efficiency and quality of the outputs.

Index Terms— night-time, hazy, dehazing, multi-scale fusion

I. INTRODUCTION

Capturing good quality outdoor images poses interesting challenges since such scenes often suffer from poor visibility introduced by weather conditions such as haze or fog. The process dehazing has been tackled using such information as rough depth [2] of the scene or multiple images [3]. More recently, several techniques [4], [5], [1], [6], [7], [8], [9], [10], [11], [12], [13], [14], have introduced solutions that do not require any additional information than the single input hazy image.

While the effectiveness of these techniques has been extensively demonstrated on daylight hazy scenes, they suffer from important limitations on night-time hazy scenes. This is mainly due to the multiple light sources that cause a strongly non-uniform illumination of the scene. Night-time dehazing has been addressed only recently [15], [16], [17]. Pei and Lee [15] estimate the airlight and the haze thickness by applying a color transfer function before applying the dark channel prior [1], [18] refined iteratively by bilateral filtering as a post-processing step. The method of Zhang et al. [16] estimates non-uniform incident illumination and performs color correction before using the dark channel prior. Li et al.[17] employ an updated optical model by adding the atmospheric point spread function to model the glowing effect. A spatially varying atmospheric light map is used to estimate the transmission map based dark channel prior.

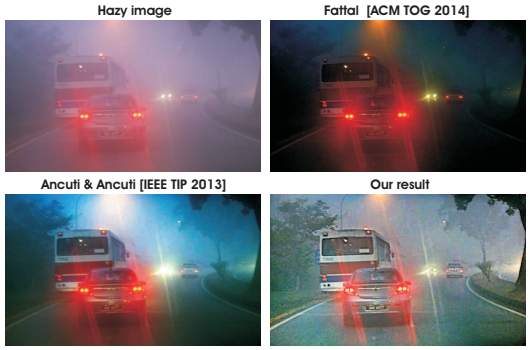

Fig. 1. *Night-time scene capture is a challenging task under difficult weather conditions and recent single-image dehazing techniques [11], [10] suffer from important limitations when applied to such images.*

We introduce a different approach to solving the problem of night-time dehazing. We develop the first fusion-based method of restoring hazy night-time images. Image fusion is a well-known concept that has been used for image editing [19], image compositing [20],image dehazing [10], HDR imaging [21], underwater image and video enhancement [22] and image decolorization [23]. The approach described here is built on our previous fusion-based daytime dehazing approach [10] that has been recently extended by Choi et al. in [24].

To deal with the problem of night-time hazy scenes (refer to Fig. 1), we propose a novel way to compute the airlight component while accounting for the non-uniform illumination presents in nighttime scenes. Unlike the well-known dark-channel strategy [18] that estimates a constant atmospheric light over the entire image, we compute this value locally, on patches of varying sizes. This is found to succeed since under night-time conditions, the lighting results from multiple artificial sources, and is thus intrinsically non-uniform. In practice, the local atmospheric light causes the color observed in hazy pixels, which are the brightest pixels of local dark channel patches. Selecting the size of the patches is non-trivial since small patches are desirable to achieve fine spatial adaptation to the atmospheric light, it might also lead to poor light estimates and reduced chance of capturing hazy pixels. For this reason, we

Part of this work has been funded by the Belgian NSF, and by a MOVE-IN Louvain, Marie Curie Fellowship.

Part of this work has been funded from Marie Curie Actions of EU-FP7 under REA grant agreement no. 600388 (TECNIOspring programme), and from the Agency for Business Competitivenness of the Government of Catalonia ACCIO : TECSPR14-2-0023.

deploy multiple patch sizes, each generating one input to the multi-scale fusion process. Our fusion approach is accomplished in three main steps. First, based on our airlight estimation using different sizes of the patches we derive the first two inputs of the fusion approach. To reduce the glowing effect and emphasize the finest details of the scene, the third input is defined to be the Laplacian of the original image. In the second step, the important features of these derived inputs are filtered based on several quality weight maps (local contrast, saturation and saliency). Finally the derived inputs and the normalized weight maps are blended in a multi-scale fashion using a Laplacian pyramid decomposition of the inputs and a Gaussian pyramid of the normalized weights.

The experimental section describes testing of our technique on a large set of different night-time hazy scenes. The results demonstrate the efficacy of our approach as compared to recent competitive techniques both in terms of computational efficiency and quality of the outputs.

II. AIRLIGHT ESTIMATION ON NIGHT-TIME HAZY SCENES

This section explains how the atmospheric factors affecting the image formation process can be estimated from night-time images formed in the presence of non-uniform (artificial) lightning. Sections II-A and II-B survey the previous art, while Section II-C introduces two original contributions.

II-A. Observation model

Due to atmospheric particles that absorb and scatter light, only a fraction of the radiance from a scene point reaches the observer. Koschmieder's model [25] is a relevant description of atmospheric effects caused by weather on the observer. In short, it states that the light intensity $\mathcal{I}$ at each image coordinate x is the result of two main additive components - *direct transmission* $\mathcal{D}$ and *airlight* $\mathcal{A}$:

$$\mathcal{I}(x) = \mathcal{D}(x) + \mathcal{A}(x) = \mathcal{J}(x)\ T(x) + A_\infty\ [1 - T(x)] \quad (1)$$

where $\mathcal{J}$ is the scene radiance or haze-free image (estimated, which would reach the observer unaltered in absence of atmospheric effects), T is the transmittivity along the cone of vision and A_∞ is the atmospheric intensity, resulting from environmental illumination.

II-B. Dark channel prior

In Koschmieder's model, the transmission map $T(x)$ is directly related to the depth of the scene. For homogeneous medium, $T(x) = e^{(-\beta\ d(x))}$ where β is the medium attenuation coefficient due to scattering, and d is the distance between the observer and the considered surface.

Following [18], and adopt the well-known dark channel (DC) prior to estimate $T(x)$ without resorting to depth estimation. The DC prior assumes that natural objects have a weak reflectance in one of the color channels (the direct radiance is small, or dark, in at least one of the R, G, B color channels [26]), while the atmospheric intensity conveys all colors (the haze looks grey or white, i.e. all components in A_∞ are significant). Hence, assuming that A_∞ is known (we discuss estimation of it later), then $T(x)$ can be directly estimated from the weakest color (relative to atmospheric color) over a neighborhood of x. Formally, under the assumption that $\min_{y\in\Omega(x)}\left(\min_{c\in r,g,b}\mathcal{J}^c/{A_\infty}^c\right) = 0$, Koschmieder's model states that:

$$T(x) = 1 - \min_{y\in\Omega(x)}\left(\min_{c\in r,g,b}\mathcal{I}^c/{A_\infty}^c\right) \quad (2)$$

where A^c_∞ is the component of the atmospheric light associated with color c, and $\Omega(x)$ represents a local patch centered at x.

II-C. Atmospheric intensity estimation

Early methods estimated the atmospheric intensity as the color vector having the highest intensity pixel [5]. This choice was motivated by the white appearance of haze in day-time scenes. Such estimate could however fail, e.g. on a white object instead of a hazy pixel. To circumvent this problem, the authors of [18] proposed to estimate the atmospheric intensity using the most haze-opaque pixels. These are defined as the ones having the brightest dark channel, i.e as the ones maximizing $I_{DC}(x) = \min_{y\in\Omega(x)}(\min_{c\in r,g,b}\mathcal{I}^c(y))$, where r, g, b denote the R,G,B color channels.

This estimator works well on day-time scenes, but suffers from two weaknesses when applied to night scenes (see Fig. 2). First, it globally estimates the atmospheric intensity, over the entire picture, whereas the night-scenes are characterized by artificial and spatially non-uniform environmental illumination. Second, by maximizing the minimum over the set of color channels, their method finds those locations taking large values in all channels. It thus implicitly assume that the atmospheric intensity is reasonably white, which is the case in day-time scenes, but is not necessarily true of night-scenes which can present strongly colored lighting.

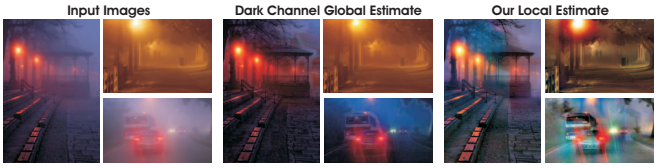

Fig. 2. **Rough dehazing of night-time scenes.** *Designed for day-time dehazing, the well-known dark channel [18] has important limitations on night scenes because it uniformly estimates the airlight constant. As may be observed, our patch-based estimate (also not refined) of the airlight component is more appropriate for the night-time hazy scenes. In particular, color and details that are close to light sources are better enhanced. By simply replacing these estimates in the model equation results in some rough dehazing outputs.*

To address those two limitations, we propose (i) to estimate the atmospheric intensity locally, within spatial neighborhoods $\Psi(x)$ around each coordinate x, and (ii) to compute each component of the atmospheric light independently. Formally, we define the local atmospheric intensity $A^c_{L\infty}(x)$ to be:

$$A^c_{L\infty}(x) = \max_{y\in\Psi(x)}\left[\min_{z\in\Omega(y)}\left(\mathcal{I}^c(z)\right)\right] = \max_{y\in\Psi(x)}\left[I^c_{MIN}(z)\right] \quad (3)$$

This formulation is again motivated by Koschmieder's model, where scene radiance $\mathcal{J}^c(x)$ can be written as $\rho^c(x).A^c_{L\infty}(x)$, with $\rho^c(x)$ denoting the normalized radiation coefficient. Maximizing independently on each color, as done in Equation 3, is equivalent to finding the coordinate y around which the normalized radiation coefficient is maximum for color c. In particular, when

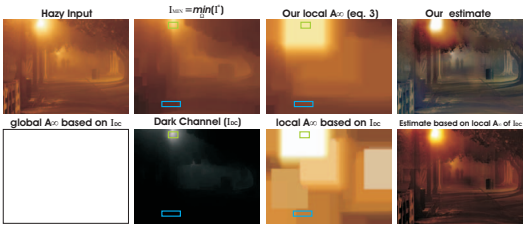

Fig. 3. **Local airlight estimation.** *A global estimate of the A_∞ based on dark channel results in a white airlight. As a consequence, the dark channel might become very small (see blue rectangle in second image of bottom row), which means $1 - T(x) \approx 0$ in Equation2 and no airlight influence in Equation 1. In contrast, our local airlight estimate on the same blue rectangle results in a colored atmospheric light, which in turns results in a non-unity transmission and a non-zero atmospheric light influence.*

an object reflects all incident color c, this coefficient is close to one at every coordinate z within neighborhood of y, and $\mathcal{I}^c(z) \approx A^c_{L\infty}(z).T(z) + A^c_{L\infty}(z).(1 - T(z)) = A^c_{L\infty}(z)$.

Obviously, each potential light source has an influence that goes beyond the size of the patch Ω used to validate the lighting relevance. Here, all results have been generated using patches Ψ twice the size of Ω.

Figure 3 compares the atmospheric intensity estimated by global and local strategies. Local estimation appears to capture the major changes arising from environmental illumination, while the global approach does not. More importantly, the bottom, rightmost pictures reveal the benefit of computing each atmospheric intensity component independently, compared to searching for the location in $\Psi(x)$ maximizing the minimum over the 3 color channels, as a straightforward locally adaptive extension of [18] would do. We also observe that the image reconstructed estimated by our local method of the atmospheric intensity is of better appearance (both in color and details) those resulting from local estimation obtained based on joint processing of the color channels.

Finally, it is worth noting that, when $\Psi(x)$ is defined to cover the entire image, our method reduces to a global estimator. Interestingly, in this case, Fig. 4 reveals that the global estimate of $A^c_{L\infty}$ derived by maximizing $\min_{y\in\Omega(x)}(\mathcal{I}^c(y))$ over the entire image is quite similar to the one proposed in [18] for day-time scenes. Hence, our proposed estimator may be regarded to be a night-friendly generalization of the concepts introduced in [18].

III. FUSION PROCESS

While a significant degree of picture enhancement is obtained using the above described local estimation procedure in the optical model, important artifacts arise at and around patch transitions, where color shifting and glowing defects are visible. Moreover, as detailed below, the choice of patch size could result in poor quality output images owing non-uniformity of the airlight in night-time scenes. To solve this problem we propose a multi-scale fusion approach which can effectively and seamlessly enhance hazy night-time images.

III-A. Inputs

Our fusion technique is a single image-based approach that uses several inputs from the original hazy image. In the first stage we employ the strategy previously described that locally estimates the airlight values. An important problem that arises is how to choose the optimal size of the patch in order to be able to deal with the case

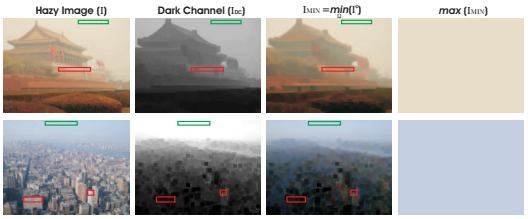

Fig. 4. **Airlight estimation**. *Our global airlight estimate $A^c_{L\infty}$, derived by maximizing $\min_{y\in\Omega(x)}(\mathcal{I}^c(y))$ over the entire image, appears to be quite similar to the atmospheric intensity estimated by He et al. [18], from the brightest region of the dark channel (depicted by green rectangles). The red rectangles show that, in daytime scenes, the two approaches equally reject the high image intensity locations that are not relevant regarding airlight estimation. He et al. [18] method rejects them because the prior is dark in those regions, our strategy because I_{MIN} gets darker than the initial image in those regions that are not subject to intense airlight illumination. Since I_{MIN} does not make any implicit assumption about the whiteness of the atmospheric illumination, it is more general than [18], especially in presence of artificial colored lighting.*

where multiple light sources are contained within the same patch. Selecting a size that is too small risks improper haze removal, effects of diffusely distributed light from a source may not be included in that patch.

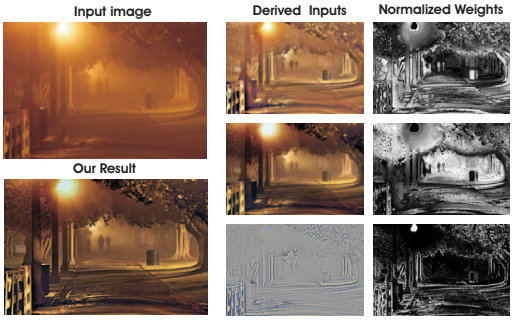

Fig. 5. *Derived inputs and corresponding normalized weight maps.*

By choosing a too large patch size the haze is better removed, but as may be seen in Fig. 5 the color might be shifted, the influence of the airlight might not be entirely removed and some details may remain poorly restored.

Based on this observations, we derive a **first** and a **second input** based on our airlight estimation using different patch sizes. The **first input** is computed using a small patch size (e.g. 20×20 for an image of size 800×600), thereby preventing estimation of the airlight from multiple light sources. However this input is characterized by an important loss of global contrast and chroma. We solve this limitation by computing a **second input** using larger patches (e.g. 80×80 for an image of size 800×600). This derived input considerably improves the global contrast, since it removes a significant fraction of the airlight. The transitions between neighboring patches is smoothed using a simple gaussian filter. When more than one light source is included in the region of interest, a winner take it all procedure decides which light source estimates the airlight.

However, as shown in Fig. 5, glowing effects are still visible in the derived inputs. To reduce such undesired effects we derive a **third input** which is the discrete Laplacian of the original image. This input makes it possible to enhance the finest details that are

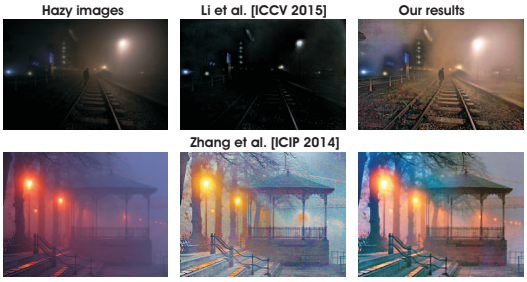

Fig. 6. *Comparative results with the recent night-time dehazing technique of Zhang et al. [16] and Li et al. [17].* **Please refer to supplementary material for more comparative results.**.

transferred to the fused output.

III-B. Weight maps

Inspired by our previous fusion dehazing approach [10], we derive three weight maps to ensure that regions of high contrast or of high saliency will receive greater emphasis in the fusion process.

Local contrast weight estimates the amount of local variation of each input and is computed by applying a Laplacian filter to the luminance of each processed image. This indicator has been used in applications such as tone mapping [21] and assigns high values to edges and texture variations.

Saturation weight map controls the saturation gain in the output image. This factor is motivated by the fact that humans generally prefer images characterized by a high level of saturation. This measure is computed as the standard deviation across channels at each coordinate.

Saliency weight map highlights the most conspicuous regions of an image compared with their surroundings. Using the well-known saliency technique of Achanta et al. [27] this weight map is computed as a difference between a Gaussian smoothed version of the input and its mean value.

III-C. Multi-scale Fusion

The main goal of the fusion process is to produce a better output image by effectively blending inputs that are guided by specific weight maps designed in order to preserve the most significant features of the inputs.

The simplest way is to directly combine the inputs and weight maps as $\mathcal{R}_{NF}(x) = \sum_k \bar{\mathcal{W}}^k(x)\mathcal{I}_k(x)$ (where $\mathcal{I}_k$ represents the k^{th} input weighted by the normalized weight maps $\bar{W}^k$). However, this naive fusion strategy has been shown to cause annoying halo artifacts, mostly at locations with strong transitions in the weight maps. Such unpleasing artifacts can be overcame by using a multi-scale Laplacian decomposition, a well-known concept dating to Burt and Adelson [28].

Similarly to other single-image dehazing approaches [10], [24], each input $\mathcal{I}_k$, is decomposed into a Laplacian pyramid while the normalized weight maps $\bar{\mathcal{W}}^k$ are decomposed using a Gaussian pyramid. Using the same number of levels, the Gaussian and Laplacian pyramids are independently fused at each level:

$$\mathcal{R}_l(x) = \sum_k G_l\left\{\bar{\mathcal{W}}^k(x)\right\} L_l\left\{\mathcal{I}_k(x)\right\} \tag{4}$$

where l represents the number of the pyramid levels, $L\{\mathcal{I}\}$ denotes the Laplacian of the input $\mathcal{I}$, and $G\left\{\bar{\mathcal{W}}\right\}$ is the Gaussian-smoothed normalized weight map $\bar{\mathcal{W}}$.

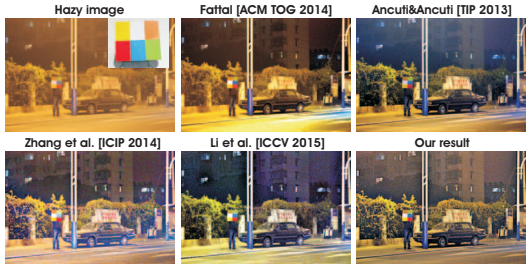

Fig. 7. **Comparative results.** *The night-time hazy image with color palette (left side, top row) is enhanced by several dehazing techniques. See Table I for the PSNR values.*

The fused result $\mathcal{R}$ is processed by summing the contributions from all the computed levels of the pyramid:

$$\mathcal{R}(x) = \sum_l \mathcal{R}_l(x) \uparrow^d \tag{5}$$

where $\uparrow^d$ is the upsampling operator with factor $d = 2^{l-1}$.

IV. RESULTS AND DISCUSSION

We extensively tested our approach using the recent image dataset introduced in [17] that contains various quality and formats of images taken of night-time scenes. We compared our method with the recent night-time dehazing techniques of Zhang et al. [16] and Li et al. [17] and also with the day-time dehazing methods of Ancuti and Ancuti [10] and Fattal [11]. For all the results we used the original code provided by the authors on their webpages.

While Fig. 1 demonstrates limitations of day-time dehazing techniques when applied to night-time hazy images, Fig. 6 directly compares our approach with the recent specialized techniques of Li et al. [17] and Zhang et al. [16]. The method of Li et al. [17] tends to darken the original image and to over-amplify colors in some regions. On the other hand, as compared with our approach, the strategy of Zhang et al. [16] is less robust to the the glowing effect and may introduce color artifacts.

Moreover, our approach has the advantage of simplicity and computational efficiency. Our unoptimized Matlab implementation processes an 800×600 image in less than 4 seconds. The method of Li et al. [17] computes results on a similar image in more than 30 seconds while the method of Zhang et al. [16] requires a similar computation as He et al. [1] (approx. 20 seconds per image).

	yellow	white	brown	red	blue	green	**average**
Fattal	21.10	23.94	15.43	20.71	15.12	15.77	18.68
Ancuti	17.75	15.82	13.49	19.16	14.01	17.01	16.20
Zhang et al.	21.20	23.21	**21.30**	20.10	15.38	12.66	18.98
Li et al.	19.80	23.21	16.94	**23.38**	**17.69**	**21.09**	20.35
Our method	**27.33**	**30.04**	18.58	23.21	17.59	17.66	**22.40**

Table I. *Evaluation of the results in Fig. 7 based on the PSNR values computed as an average on RGB components for each of the 6 colors of the reference palette.*

We also performed a quantitative evaluation using the pair of images provided by Zhang et al. [16]. On the left side of the top row of Fig. 7 is shown the reference color palette and the night-time hazy image containing the same palette. We processed this input image using several different dehazing techniques [10], [11], [16], [17] and computed the PSNR values for each of the 6 colors (shown in Table I). As can be seen, our approach generally performs better in terms of PSNR compared with the other techniques.

V. REFERENCES

[1] K. He, J. Sun, and X. Tang, "Single image haze removal using dark channel prior," *In IEEE CVPR*, 2009.

[2] J. Kopf, B. Neubert, B. Chen, M. Cohen, D. Cohen-Or, O. Deussen, M. Uyttendaele, and D. Lischinski, "Deep photo: Model-based photograph enhancement and viewing," in *Siggraph ASIA, ACM Trans. on Graph.*, 2008.

[3] S.G. Narasimhan and S.K. Nayar, "Contrast restoration of weather degraded images," *IEEE Trans. on Pattern Analysis and Machine Intell.*, 2003.

[4] R. Fattal, "Single image dehazing," *SIGGRAPH*, 2008.

[5] R. T. Tan, "Visibility in bad weather from a single image," *In IEEE Conference on Computer Vision and Pattern Recognition*, 2008.

[6] J.-P. Tarel and N. Hautiere, "Fast visibility restoration from a single color or gray level image," *In IEEE ICCV*, 2009.

[7] L. Kratz and K. Nishino, "Factorizing scene albedo and depth from a single foggy image," *ICCV*, 2009.

[8] C. O. Ancuti, C. Ancuti, and P. Bekaert, "Effective single-image dehazing by fusion," in *In IEEE ICIP*, 2010.

[9] C. O. Ancuti, C. Ancuti, C. Hermans, and P. Bekaert, "A fast semi-inverse approach to detect and remove the haze from a single image," *ACCV*, 2010.

[10] C.O. Ancuti and C. Ancuti, "Single image dehazing by multi-scale fusion," *IEEE Transactions on Image Processing*, vol. 22(8), pp. 3271–3282, 2013.

[11] R. Fattal, "Dehazing using color-lines," *ACM Trans. on Graph.*, 2014.

[12] C. Ancuti and C. O. Ancuti, "Effective contrast-based dehazing for robust image matching," *IEEE Geoscience and Remote Sensing Letters*, 2014.

[13] S. Emberton, L. Chittka, and A. Cavallaro, "Hierarchical rank-based veiling light estimation for underwater dehazing," *Proc. of British Machine Vision Conference (BMVC)*, 2015.

[14] K. Tang, J. Yang, and J. Wang, "Investigating haze relevant features in a learning framework for image dehazing," *IEEE CVPR*, 2009.

[15] S. C. Pei and T.Y. Lee, "Nighttime haze removal using color transfer pre-processing and dark channel prior," *In IEEE Int. Conf. Image Processing*, 2012.

[16] J. Zhang, Y. Cao, and Z. Wang, "Nighttime haze removal based on a new imaging model," *In IEEE Int. Conf. Image Processing*, 2014.

[17] Y. Li, R. T. Tan, and M. S. Brown, "Nighttime haze removal with glow and multiple light colors," *In IEEE Int. Conf. on Computer Vision*, 2015.

[18] K. He, J. Sun, and X. Tang, "Single image haze removal using dark channel prior," *IEEE Trans. on Pattern Analysis and Machine Intell.*, 2011.

[19] P. Perez, M. Gangnet, and A. Blake, "Poisson image editing," *ACM Trans. Graph (SIGGRAPH)*, 2003.

[20] M. Grundland, R. Vohra, G. P. Williams, and N. A. Dodgson, "Cross dissolve without cross fade," *Computer Graphics Forum*, 2006.

[21] T. Mertens, J. Kautz, and Frank Van Reeth, "Exposure fusion," *Comp. Graph. Forum*, 2009.

[22] C. Ancuti, C. O. Ancuti, T. Haber, and P. Bekaert, "Enhancing underwater images and videos by fusion," in *IEEE Conference on Computer Vision and Pattern Recognition (CVPR)*, 2012.

[23] C. O. Ancuti, C. Ancuti, C. Hermans, and P. Bekaert, "Image and video decolorization by fusion," *Asian Conference on Computer Vision*, 2010.

[24] L. K. Choi, J. You, and A. C. Bovik, "Referenceless prediction of perceptual fog density and perceptual image defogging," *IEEE Trans. on Image Processing*, vol. 24, no. 10, 2015.

[25] H. Koschmieder, "Theorie der horizontalen sichtweite," in *Beitrage zur Physik der freien Atmosphare*, 1924.

[26] P.S. Chavez, "An improved dark-object subtraction technique for atmospheric scattering correction of multispectral data," *Remote Sensing of Environment*, 1988.

[27] R. Achantay, S. Hemamiz, F. Estraday, and S. Susstrunk, "Frequency-tuned salient region detection," *IEEE CVPR*, 2009.

[28] P. Burt and T. Adelson, "The laplacian pyramid as a compact image code," *IEEE Transactions on Communication*, vol. 31, no. 4, 1983.